Chapter 28
Air Photonics: Tera – Mid Infrared Radiation

X.-C. Zhang

Abstract Air, especially ionized air (plasma), has been used to generate intense peak THz waves (THz field $>$ 2.5 MV/cm) with a broadband spectrum (10% bandwidth covers entire THz gap, and extends into mid-IR range). Remote sensing using air as THz wave emitter and sensor is demonstrated.

28.1 Introduction

Since the first demonstration of THz wave time-domain spectroscopy in the late 1980s, there has been a series of significant advances of THz wave sensing and spectroscopic imaging. The development of intense THz sources and more sensitive detectors provide new opportunities for understanding the basic science in the THz frequency range. As THz wave technology improves, new THz wave sensing and imaging capabilities impact a range of interdisciplinary fields. This is particularly crucial for non-destructive evaluation (immediate application), national security (3–5 years), and medical diagnosis or even clinical treatment in biomedical applications (5–10 years) [1].

Recent advances of THz air photonics include the development of broadband THz wave (10% bandwidth at 0.1 THz to 46 THz), covers from THz to mid IR. The intense THz field ($>$1 MV/cm), THz wave generation at standoff distance, and remote sensing of THz signal by using radiation-enhanced-emission-of-fluorescence (REFF) in air, are the examples of closing the THz gap between theory, development and application.

X.-C. Zhang
Center for Terahertz Research,
Rensselaer Polytechnic Institute, Troy, NY 12180, USA

M.F. Pereira and O. Shulika (eds.), *Terahertz and Mid Infrared Radiation*: *Generation, Detection and Applications*, NATO Science for Peace and Security Series B: Physics and Biophysics, DOI 10.1007/978-94-007-0769-6_28,

28.2 THz Generation Using Air Plasma

THz sensing and imaging is a cutting edge technology. Standoff detection with THz waves is one of the most challenging and desired research topics in remote sensing. Most research and development efforts on active detection are limited to a short distance (10 m or less), this is due to the water vapor attenuation in the THz frequency range and the insufficient THz power. Passive THz detection has its great advantages – it is non-invasive, truly standoff, and safe; however, its limitation is the inability to provide spectroscopic measurement and it strongly depends on the background environment. Using air as the THz emitter and sensor near the target(s) with laser excitation provides a feasible approach for standoff detection. Recently we have demonstrated THz field generation at a distance greater than 30 m, as shown in Fig. 28.1. This demonstration was a crucial step toward the goal of standoff THz wave generation.

When a high-energy ($>\sim 100\,\mu J$), ultrafast laser pulse is focused in a gaseous medium, broadband terahertz radiation is emitted. When the laser pulse is combined with another pulse at its second harmonic, the emission is dominated by nonlinear optical processes similar to four-wave mixing [2]. Several THz wave emission mechanisms, including the perturbation approach commonly used in nonlinear optics, classical treatment and semi-classical carrier dynamics, have been proposed. At optical intensities in the range of $10^{14}\,W/cm^2$ and above, there is significant ionization of the medium, accompanied by a dramatic increase in the observed THz emission. Multiple semi-classical models fail to describe important aspects of this phenomenon, either quantitatively or qualitatively. Solving the time-dependent Schrödinger equation is the key to understand intense broadband THz wave generation and detection in gases [4]. In principle, this calculation gives a detailed explanation of the experimental work and offer insight into the ultrafast electron dynamics involved, from ionization to collision.

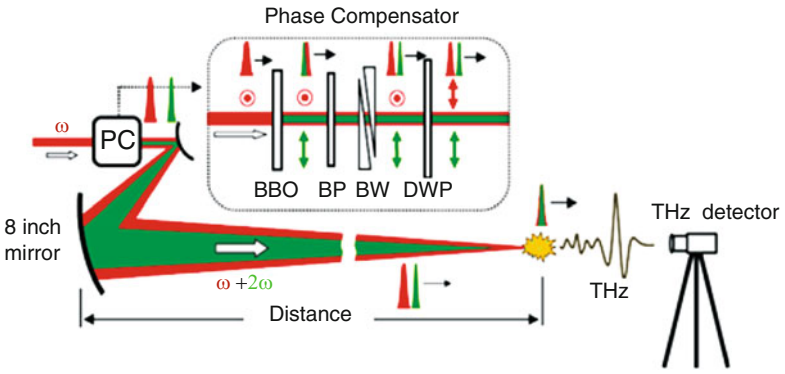

Fig. 28.1 Schematic illustration of the experimental setup for remote THz wave generation from laser-induced air plasma: The middle panel shows the THz waveform generated at a distance of over 17 m, with total laser pulse energy of about 550 μJ and pulse duration of about 100 fs at a repetition rate of 1 kHz. 17 m is the full length of our THz lab. The phase compensator is a crucial element for the standoff generation

A systematic study of the THz waves radiated during the formation of the laser-induced plasma yields a wealth of information about how coherent effects during the very fast and microscopic tunnel ionization process translate into coherent effects in the macroscopic plasma, a transition which is difficult to study in any other region of the spectrum.

28.3 Phase and Polarization Control

Theoretically, the electrons exhibit different trajectories after being ionized from an atom or molecule by circularly or elliptically polarized optical pulses (ω plus 2ω), in comparison to the case when the pulses are linearly polarized. However, no theoretical predication has been specified for the case of THz generation with circularly or elliptically polarized two-color excitation (ω and 2ω beams), although a semi-classical model to the case with circularly polarized, single-color, few-cycle optical excitation was proposed before. Using the quantum mechanical model described in our previous work, we calculated the electron expectation value trajectories in the case of circularly and elliptically polarized ω and 2ω beams. When linearly polarized optical excitation is used, the problem essentially reduces to two dimensions, and one expects the THz radiation to share the polarization of the pump pulses.

When circularly or elliptically polarized optical fields are applied, the laser-atom interaction requires three dimensions, since the optical field is capable of coupling states with differing values of the z-projection of the angular momentum (m) in addition to the angular momentum l. This was calculated by representing the electron wave function as a series of partial waves in spherical coordinates, with a spatial radial dimension and momentum-space angular dimensions, and numerically solving the time-dependent Schrödinger equation. The simulations can initially be done using hydrogen for simplicity. The system of coordinates was rotated dynamically such that the vector potential of the laser was always aligned with the z-axis (the laser Poynting vector was along the y-axis), which allowed the m-coupling to be confined to a single operation, $\exp(i\theta L_y)$. The exact (real, dense) operator was used rather than the infinitesimal or Padé approximants so that arbitrary ellipticities could be utilized without the build-up of rotation errors. The laser-induced coupling between the l partial waves was performed in the velocity gauge. The two-dimensional electron polarization was continuously monitored throughout the simulation by calculating the expectation values $\langle \mathrm{z} \rangle$ and $\langle \mathrm{x} \rangle$ at each time step.

This polarization completely describes the THz radiation produced by the first step of the THz emission process (ionization), and also determines the direction of the remaining emission processes [5]. The 3D quantum mechanical simulation in Fig. 28.2 plots the consequence of changing the relative phase between the fundamental and second harmonic carrier waves, ϕ, when the optical pulses are both right-circularly polarized. We can see that instead of the intensity modulation observed with linearly polarized excitation, the THz intensity remains constant, but the polarization angle rotates with ϕ.

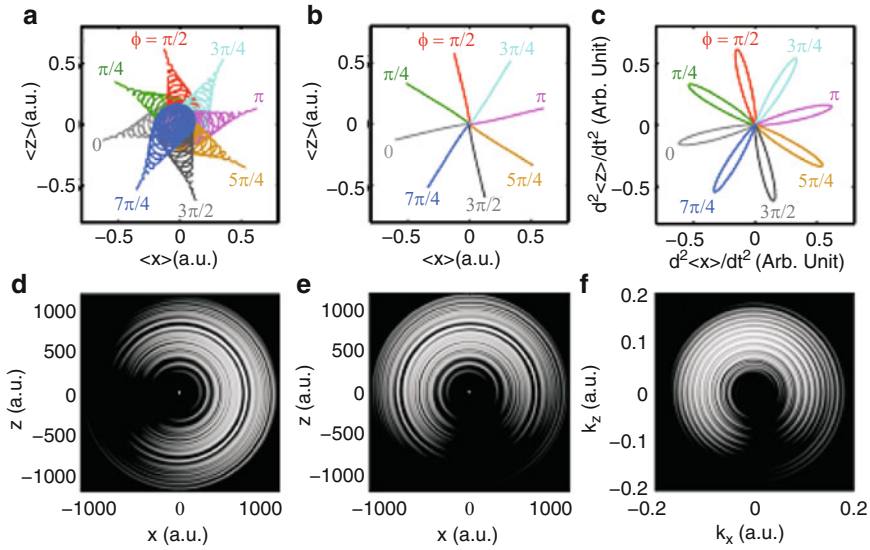

Fig. 28.2 (a) Electron expectation value trajectories in the dual-color field. (b) Electron trajectories with the laser-driven quiver motion removed. (c) Second time-derivative of the trajectories, showing the effective polarization of the emitted radiation. (d) and (e) Final electron density distribution in the z-x plane (scaled logarithmically) for the phases π and $\pi/2$ respectively. (f) Momentum space electron density distribution for phase $\pi/2$ (scaled logarithmically, bound states removed)

Motivated by the above physical picture and some preliminary experimental results indicating that the THz electric-field detected by polarization-sensitive electric-optic sampling does not increase when the THz power detected with a pyroelectric detector is tripled during the optimization of the THz emission, we performed systematic experiments to test the polarization behavior of THz waves generated from gas plasma. We performed both theoretical and experimental investigations of the THz polarization characteristics as the relative phase between the ω and 2ω pulses changes, with different combinations of the polarizations of the two pulses.

The polarization of the THz waves is coherently controllable through the phase when at least one of the optical pulses (ω or 2ω) is elliptically polarized. In particular, when both ω and 2ω beams are circularly polarized (or close to it), the THz polarization angle can be rotated arbitrarily simply by changing the phase, with the THz amplitude kept unchanged. Our results not only give a clearer picture about the behavior of the THz emission from gas plasma but also add to the THz air source a more attractive feature that may lead to fast THz wave modulation devices and enable coherent control of nonlinear responses excited by intense THz waves.

In order to test the theoretical predictions, a stable phase control mechanism with 10 s of attosecond accuracy and sufficient scan range is necessary. Instead of using a glass plate as the phase compensator, a new phase compensator in an in-line configuration with attosecond phase-control accuracy is employed, as shown inside the dashed line in Fig. 28.3(a). A femtosecond pulse at 800 nm (ω) generates

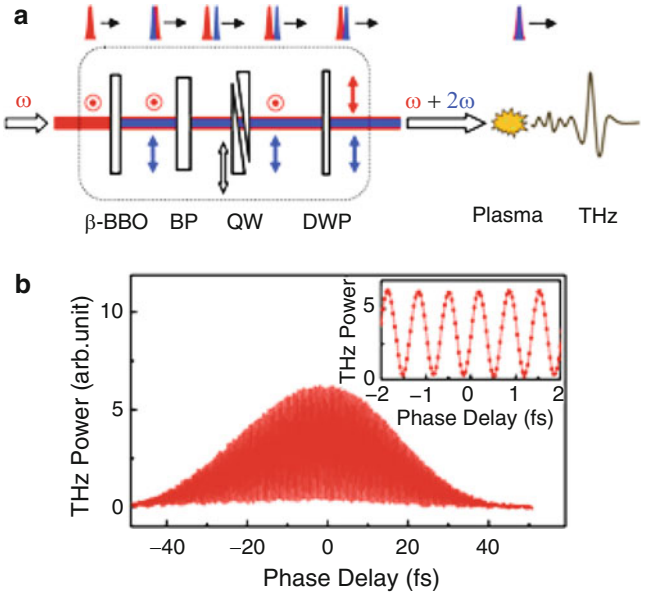

Fig. 28.3 (a) Schematic illustration of the experimental setup. Inside the dashed line is the in-line phase compensator. β-BBO, Beta Barium Borate crystal; BP, Birefringent Plate (α-BBO); QW, Quartz Wedges; DWP, Dual-wavelength Waveplate; the red and blue arrows indicate the polarization of the ω and 2ω beams, respectively. (b) A typical phase curve obtained by changing relative phase between the ω and 2ω pulses through the change of the insertion of one of the wedges while monitoring the THz average power with a pyroelectric detector when the ω and 2ω pulses are linearly polarized and parallel to each other; the inset shows a zoomed-in portion of the phase curve. Sub-femtosecond stability of optical phase control is necessary

a second harmonic pulse at 400 nm (2ω) while passing through a type-I Beta Barium Borate (β-BBO) crystal. The ω and 2ω beams, which have perpendicular polarizations, pass through an x-cut birefringent plate (BP, here we suggest α-BBO) with its slow axis aligned with the ω beam polarization (o-ray) and the fast axis aligned with the 2ω beam (e-ray) so that right after this plate the 2ω pulse leads the ω pulse, as shown in the figure. A fused silica wedge pair is used to finely control the phase delay between the ω and 2ω pulses through the relationship $\triangle\tau = \triangle l(n_{2\omega} - n_{\omega})\tan(\theta_{\omega})$, where $\triangle l$ is the step size of the mechanical translation stage, n_{ω} and $n_{2\omega}$ are the refractive indices of the fused silica at 800 nm and 400 nm, respectively, θ_{ω} is the wedge angle, and $\triangle\tau$ is the resulting optical delay step. Finally, a tunable dual-band waveplate is used to control polarizations of the ω and 2ω beams.

The advantage of this in-line phase compensator is that it combines minimal lateral displacement and the minimal phase fluctuation of the phase plate. Both ω and 2ω beams are focused to ionize the gas and emit THz waves. A broadband THz polarizer is used to analyze the polarization of the emitted THz waves, and a pyroelectric detector is used to monitor the transmitted THz power through the THz

polarizer as it rotates. Figure 28.3(b) shows a phase curve obtained by changing the phase between ω and 2ω pulses through the translation of one wedge while monitoring at the THz power with a pyroelectric detector when ω and 2ω pulses are linearly polarized and parallel to each other. 10 s of attosecond stability of optical phase control is achieved.

28.4 THz Detection by Using Radiation-Enhanced-Emission-of-Fluorescence (REEF)

Previously, we have developed THz air-biased-coherent-detection (THz ABCD) [3]. THz ABCD is an excellent point detection method with ultra-wide bandwidth, high sensitivity, and coherent capability. However, the drawback is the local detection only.

To gain a full control of THz detection at standoff distance, we study the interaction between a THz pulse and plasma by measuring radiation-enhanced-emission-of-fluorescence (REEF) [6]. Laser induced plasma in air could emit fluorescence in 300–400 nm (nitrogen lines). It is a good start with a semi-classical modeling of electron motion in the presence of the THz field and electron-impact-excitation of gas molecules in the calculation of the dynamics of time-dependent plasma response to the THz pulse as a function of electron collision relaxation time and electron-ion recombination rate. The enhanced fluorescence emission should be quadratically dependent on the THz field. We demonstrate coherent detection of broadband THz waves by measuring THz REEF from laser-induced plasma ($>$10 m) in ambient air. Unlike other widely used THz detection techniques, this method should provide an omni-directional emission pattern.

Under the influence of THz radiation, the electron dynamics in laser-induced plasma are determined by the amplitude and phase of the laser pulse and THz pulse, their delay and the gas density. Intense illumination by an ultrashort laser pulse releases free electrons from air molecules by multi-photon ionization or tunneling ionization processes.

To test the semiclassical model of THz-REEF, we experimentally investigated the influence of the THz pulse on the plasma. The schematic of the experimental set-up is shown in Fig. 28.4(a). A broadband, single-cycle of free space THz radiation with linear polarization and a peak field of 100 kV/cm, generated from a Lithium Niobate prism using the tilted pulse front scheme, is focused into a plasma region which is formed by focusing a 100 μJ femtosecond laser pulse with a center wavelength of 800 nm. The laser pulses propagate collinearly with the THz pulses. The plasma fluorescence spectrum is measured by a monochromator and a photo multiplier tube (PMT).

The influence of the THz field on the laser-induced plasma emission spectrum is experimentally investigated in the spectral range of 320–400 nm which contains the strongest fluorescence emission of nitrogen gas. Figure 28.4(b) shows that fluorescence emission from both nitrogen molecules and ions are enhanced by the same

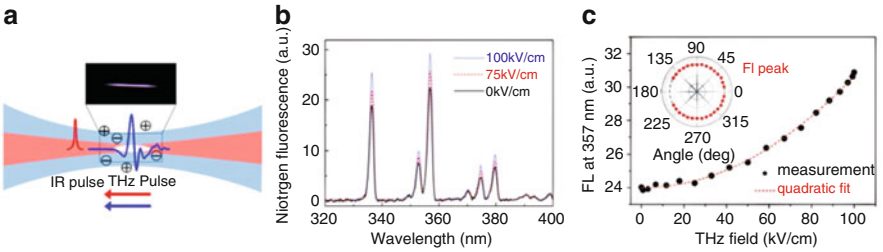

Fig. 28.4 (a) Schematics of the interaction between the THz wave and laser-induced plasma. (b) The measured fluorescence spectra in the range of 320 nm and 400 nm versus THz field. (c) The measured quadratic THz field dependence of 357 nm fluorescence emission line. Inset: The isotropic emission pattern of THz-REEF

factor as THz field is increased. In Fig. 28.4(c), we show that the measured THz field dependence of the total emission FL at the strongest line (357 nm) and the quadratic fit. $\triangle FL$ is proportional to the THz intensity at all wavelengths at ambient pressure. In the inset of Fig. 28.4(c), the angular pattern of fluorescence shows an isotropic emission profile. These observations indicate that the THz pulse enhances rather than quenches plasma fluorescence emission and further imply that photo-ionized electrons gain kinetic energy from the THz field through electron inverse-bremsstrahlung heating by the THz pulse, resulting in transfer kinetic energy to air molecules/ions via collisions.

These observations indicate that the THz pulse enhances rather than quenches plasma fluorescence emission and further imply that after electrons are heated by the THz radiation, electron-impact-excitation promotes a fraction of the gas species into upper electronic states that decay and emit fluorescence. Therefore, studying the subsequent molecular fluorescence emission provides information of electron temperature, energy transfer from electron to molecules and population of excited molecular states in the presence of the THz radiation.

As a function of the time delay between the THz pulse and the gas-ionizing laser pulse, THz enhanced fluorescence carries the information of THz time domain waveform. Utilizing the quadratic field dependence at ambient pressure and heterodyne detection method, REEF could be used for broadband coherent THz detection. The temporal resolution of detected THz pulse is determined by the ionizing pulse envelope. Figure 28.5(a) shows the time domain THz waveforms measured using the REEF in dry nitrogen and ambient air. The sharp water molecules absorption lines were presented in THz spectrum in Fig. 28.5(b). To demonstrate the capability of THz spectroscopy using REEF, we measured the transmitted THz spectrum of a 4A-DNT explosive pellet sample. Figure 28.5(c) plots the absorption features of 4A-DNT at 0.5 THz and 1.25 THz by measured REEF. This spectral result is in excellent agreement to spectral signatures resolved by electro-optic (EO) sampling. This agreement confirms the capability of THz REEF to spectrally resolve the molecular absorption signature.

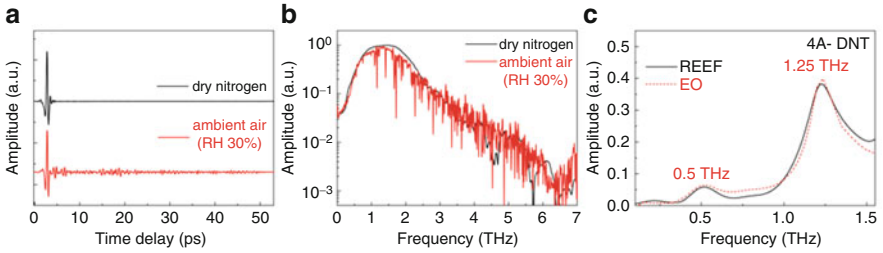

Fig. 28.5 (a) The THz waveforms measured by the THz REEF in dry nitrogen and ambient air. (b) The corresponding THz spectra of the waveforms in (a). (c) The THz absorption spectroscopy of 4A-DNT explosive sample measured by THz-REEF and EO sampling. The good agreement confirms the capability of THz REEF to spectrally resolve the molecular absorption signature (both in vapor and in solid phases)

Unlike other widely-used THz detection techniques, this method is characterized by an omni-directional emission pattern and a THz signal that is encoded in gas fluorescence which can propagate through air for kilometers without suffering too much ambient absorption. These merits make THz-REEF a promising tool for molecular recognition at standoff distance.

Acknowledgements The author gratefully acknowledges support from the National Science Foundation, Defense Threat Reduction Agency, and the Department of Homeland Security through the DHS-ALERT Center under Award No. 2008-ST-061-ED0001. The views and conclusions contained in this document are those of the authors and should not be interpreted as necessarily representing the official policies, either expressed or implied, of the U.S. Department of Homeland Security.

References

[1] B. Ferguson and X.-C. Zhang, "Materials for Terahertz Science and Technology," Review Article, Nature Materials, 1, 26 (2002).
[2] Xu Xie, Jianming Dai, and X.-C. Zhang, "Coherent control of THz wave generation in ambient air," Phys. Rev. Letts., 96, 075005 (2006).
[3] Jianming Dai, Xu Xie, and X.-C. Zhang, "Detection of broadband terahertz waves with laser-induced plasma in gases," Phys. Rev. Letts, 97, 103903 (2006).
[4] Nicholas Karpowicz and X.-C. Zhang, "Coherent Terahertz Echo of Tunnel Ionization in Gases," Phys. Rev. Letts., 102, 093001 (2009).
[5] Jianming Dai, Nicholas Karpowicz, and X.-C. Zhang, "Coherent polarization control of terahertz waves generated from two-color laser-induced gas plasma," Phys. Rev. Lett. 103, 023001 (2009).
[6] Jingle Liu and X.-C. Zhang, "Terahertz radiation-enhanced-emission-of-fluorescence from gas plasma," Phys. Rev. Lett. 103, 235002 (2009).